IL NUOVO CIMENTO **38 C** (2015) 75
DOI 10.1393/ncc/i2015-15075-4

COMMUNICATIONS: SIF Congress 2014

Tilted and standard ring solitons in shallow water

A. MANNAN(*)

Dipartimento di Matematica e Fisica, Seconda Università degli Studi di Napoli, Caserta, Italy
INFN, Sezione di Napoli, Complesso Universitario Monte Sant'Angelo, Napoli, Italy

received 24 February 2015

Summary. — The propagation of nonlinear multiring soliton structures in a shallow water is theoretically investigated. To study this problem, we have derived a cylindrical (or concentric) Korteweg-deVries equation (cKdVE) for an incompressible, inviscid, and irrotational fluid. The cKdVE has been solved analytically and numerically to describe, respectively, the localized multiring structures with tilted and standard boundary conditions.

PACS 92.10.Hm – Ocean waves and oscillations.
PACS 05.45.Yv – Solitons.
PACS 02.30.Jr – Partial differential equations.

1. – Introduction

Water waves exhibit some basic features which can be rarely matched by other kinds of waves that are found in nature. They can be perceived qualitatively with attentive naked eyes. It is also a remarkable fact that several mathematical techniques used to analyze and solve the nonlinear partial differential equations have been developed for the first time in water wave physics. Later on, they were transferred to the other disciplines, such as nonlinear optics, plasma physics, condensed matter physics, electrical transmission lines, etc. Valuable examples are the very massive applications of nonlinear equations, such as Korteweg-de Vries equation (KdVE), nonlinear Schrödinger equation (NLSE) and Kadomtsev-Petviashvili equation (KPE), to the above disciplines [1-6]. Furthermore, it is worth noting that water wave physics in the nonlinear regime is related not only to the natural occurrence of extreme events [7,6], such as the rogue wave [8,9] and the tsunami generation [10], but it includes also the study of artificially produced nonlinear wave phenomena [11] that are of great interest in physical oceanography and environmental risk studies [6].

(*) Email: mannan_phys@yahoo.com

In this paper, we present a theoretical investigation on the nonlinear propagation of ring-type multisoliton in shallow water that has been recently carried out [12]. We consider the model of an incompressible, inviscid, irrotational water described by the set of Euler's fluid equations. In cylindrical geometry and using a method of multiple scales for weakly nonlinear and dispersive waves, this set of equations is suitably reduced to the cylindrical (*i.e.* concentric) Korteweg-de Vries equation (cKdVE) that governs the propagation of nonlinear ring waves. We look for both analytical and numerical localized solutions that result from the free fall of an initially given multiring soliton in shallow water. The analytical solutions satisfy "tilted" boundary conditions, *i.e.* they are localized structures living on an oblique asymptote. The numerical solutions satisfy "standard" boundary conditions, *i.e.* they are localized structures whose wings vanish asymptotically in the space-like domain. We provide a $(1+1)$D representation and adopt a pair of spatiotemporal dimensionless coordinates, say R and T, that represent the space-like propagation coordinate and the time, respectively [13]. Then, we express these solutions by means of a $(2+1)$D representation, where R is expressed in terms of the Cartesian horizontal coordinates, say, X and Y ($R=\sqrt{X^2+Y^2}$), while the time-like variable is still T [13].

2. – Model description

The water is regarded as an incompressible, irrotational, inviscid fluid, with a zero surface tension and with density ρ. It lies on an impermeable bed, with constant depth and with a constant atmospheric pressure at the free surface. One can reduce the set of fluid equations in cylindrical symmetry to the following cylindrical (or concentric) Korteweg-de Vries equation (cKdVE) using the method of multiple scales (for details, see refs. [14, 15]):

$$\frac{\partial H_0}{\partial s}+\frac{3}{2}H_0\frac{\partial H_0}{\partial \zeta}+\frac{1}{6}\frac{\partial^3 H_0}{\partial \zeta^3}+\frac{H_0}{2s}=0, \tag{1}$$

where ζ and s are the dimensionless stretched space-like and time-like variables, respectively, and H_0 is the rescaled leading order term of the elevation expansion (for details see ref. [14]). Note that, the last term of eq. (1), *i.e.*, $H_0/2s$ comes from the cylindrical geometry adopted in our description. If we formally remove this term, eq. (1) reduces to the planar KdVE (pKdVE) (see eq. (4)).

We perform the following transformation:

$$\zeta(R,T)=R-T, \quad s(R,T)=T, \text{ and } v(R,T)=H_0(\zeta(R,T),s(R,T)), \tag{2}$$

where T and R ($0<T<\infty$, $0\leq R<\infty$) play the role of the time and the space-like coordinates, respectively. The latter conforms to the propagation (or, more precisely, to the expansion) along the radial direction [13], respectively. Using these transformations, we reduce eq. (1) in the following form [12]:

$$\frac{\partial v}{\partial T}+\frac{\partial v}{\partial R}+\frac{3}{2}v\frac{\partial v}{\partial R}+\frac{1}{6}\frac{\partial^3 v}{\partial R^3}+\frac{v}{2T}=0. \tag{3}$$

Equation (3) governs the spatiotemporal evolution of cylindrical, ring-type, multisoliton solutions in the (R,T) domain.

3. – Analytical multisoliton solution of cKdVE

A class of analytical solutions of cKdVE has been obtained from the solutions of KdVE by employing the appropriate transformations of variables [12]. Let us write the pKdVE for the leading order term of the elevation expansion, say, η_0 as the following form:

$$\frac{\partial \eta_0}{\partial \tau} + \frac{3}{2}\,\eta_0 \frac{\partial \eta_0}{\partial \xi} + \frac{1}{6}\frac{\partial^3 \eta_0}{\partial \xi^3} = 0. \tag{4}$$

If $\eta_0(\xi,\tau)$ is solution of eq. (4), then the function

$$H_0(\zeta, s) = s^{-1}\left[\eta_0\left(\xi = s^{-1/2}\zeta, \tau = -2s^{-1/2}\right) + \zeta/3\right] \tag{5}$$

is solution of eq. (1) [16,17]. By using the transformations (2), $H_0(\zeta, s)$ easily becomes:

$$v\,(R,T) = \frac{1}{T}\left[\eta_0\left(\frac{R-T}{T^{1/2}}, -\frac{2}{T^{1/2}}\right) + \frac{R-T}{3}\right]. \tag{6}$$

Since we are also going to show the solution v in the form of a ring structure through the horizontal variables X, Y at each time T, eq. (6) can be cast as

$$v\,(X,Y,T) = \frac{1}{T}\left[\eta_0\left(\frac{\sqrt{X^2+Y^2}-T}{T^{1/2}}, -\frac{2}{T^{1/2}}\right) + \frac{\sqrt{X^2+Y^2}-T}{3}\right], \tag{7}$$

where we have used the relation $R = \sqrt{X^2+Y^2}$. Note that, if η_0 satisfies the standard boundary conditions, *i.e.* $\eta_0\,(\xi,\tau) \to 0$ when $\xi \to \pm\infty$, then it is obvious from eq. (6) that $v\,(R,T)$ is the superposition of a localized structure and a straight line in the (R,T) domain. The straight line, which also plays the role of asymptote, is given by: $R/3T - 1/3$; then its slope decreases as $1/T$. Consequently, at each T, $v\,(R,T)$ is a localized structure whose wings fit to the oblique asymptote: $v = R/3T - 1/3$; then, we refer v to as *tilted* localized structure because it satisfies the *tilted* boundary conditions. It is worth noting that, for $T \to \infty$, we have $v \to -1/3$, *i.e.* as the time increases, the tilted soliton gradually flattens, reaching a flat profile for asymptotic times.

3˙1. *One-soliton solution.* – To follow the above procedure, we find the analytical one-soliton solution of eq. (1) as the image of the one-soliton solution of the KdVE, given by $\eta_0(\xi,\tau) = u_{m0}\,\mathrm{sech}^2\left[\sqrt{3u_{m0}/4}\,(\xi - V_0\tau)\right]$, where $V_0 = u_{m0}/2$. Therefore, we call *tilted soliton* the corresponding solution of cKdVE. Therefore, a tilted one-soliton solution of eq. (1) is given by [16,17]

$$H_0(\zeta, s) = \frac{1}{s}\left\{\frac{\zeta}{3} + u_{m0}\,\mathrm{sech}^2\left[\sqrt{\frac{3\,u_{m0}}{4\,s}}\,(\zeta + u_{m0})\right]\right\}, \tag{8}$$

where u_{m0} is the maximum amplitude of the corresponding planar soliton. Then, we rewrite the solution (8) in terms of the new variables R and T, obtaining

$$v(R,T) = \frac{1}{T}\left\{\frac{1}{3}\,(R-T) + u_{m0}\,\mathrm{sech}^2\left[\sqrt{\frac{3\,u_{m0}}{4\,T}}\,[(R-T) + u_{m0}]\right]\right\}. \tag{9}$$

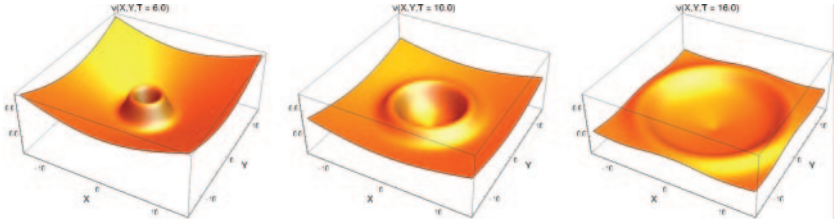

Fig. 1. – Analytical spatial profile of the ring-type bright soliton in (X, Y, T) domain at fixed values of T and $u_{m0} = 3.5$.

Figure 1 shows the spatiotemporal evolution of the tilted ring-type bright soliton in the (X, Y, T) domain at fixed values of T. We observe that, as T increases, the pulse profile propagates circularly outward and, according to eq. (9), as T increases, both the amplitude of the soliton pulse and the slope of the oblique asymptote decrease; whilst, the width of the pulse increases. However, the pulse preserves its soliton shape during this evolution.

3˙2. *Two- and three-soliton solutions.* – By applying the same transformations (2) to the two- and three-soliton solutions of KdVE, we also easily find the analytical tilted solutions of eq. (3) in the form of bright two- and three-tilted solitons, respectively:

$$v(R,T) = \frac{1}{T}\left[\frac{R-T}{3} + (u_{m2}-u_{m1})\frac{P'+Q'}{S'^2}\right], \tag{10}$$

$$v(R,T) = \frac{1}{T}\left[\frac{R-T}{3} + P' - (u_{m2}-u_{m3})\,\frac{W'}{\left(\frac{u_{m1}-u_{m2}}{S'} - \frac{u_{m3}-u_{m1}}{T'}\right)^2}\right], \tag{11}$$

where

$$S' = \sqrt{u_{m1}}\tanh\left[\sqrt{\frac{3\,u_{m1}}{4\,T}}\,(R-T+u_{m1})\right] - \sqrt{u_{m2}}\coth\left[\sqrt{\frac{3\,u_{m2}}{4\,T}}\,(R-T+u_{m2})\right],$$

$$P' = u_{m1}\,\mathrm{sech}^2\left[\sqrt{\frac{3\,u_{m1}}{4\,T}}\,(R-T+u_{m1})\right],\; Q' = u_{m2}\,\mathrm{cosech}^2\left[\sqrt{\frac{3\,u_{m2}}{4\,T}}\,(R-T+u_{m2})\right],$$

$$W' = \frac{(u_{m2}-u_{m1})\,(P'+Q')}{S'^2} + \frac{(u_{m3}-u_{m1})\,(R'-P')}{T'^2},$$

$$R' = u_{m3}\,\mathrm{sech}^2\left[\sqrt{\frac{3\,u_{m3}}{4\,T}}\,(R-T+u_{m3})\right],$$

$$T' = \sqrt{u_{m3}}\tanh\left[\sqrt{\frac{3\,u_{m3}}{4\,T}}\,(R-T+u_{m3})\right] - \sqrt{u_{m1}}\,\tanh\left[\sqrt{\frac{3\,u_{m1}}{4\,T}}(R-T+u_{m1})\right].$$

Figures 2 and 3 display the spatiotemporal evolution of the two-tilted and three-tilted soliton solution, respectively, in the (X, Y, T) domain, at fixed values of T, according to eq. (7).

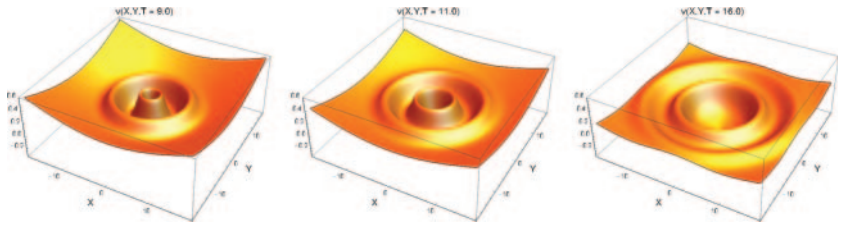

Fig. 2. – Analytical spatial profile of the ring-type two-soliton in (X, Y, T) domain at fixed values of T and $u_{m1} = 3.0$, $u_{m2} = 5.5$.

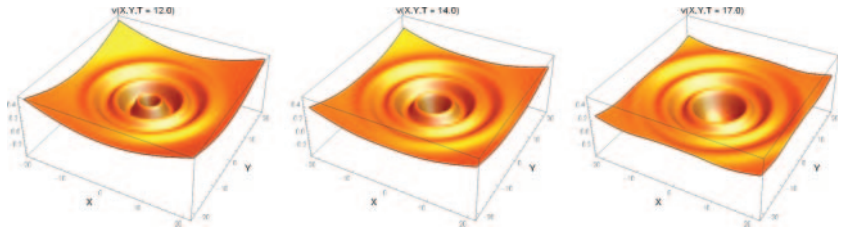

Fig. 3. – Analytical spatial profile of the ring-type three-soliton in (X, Y, T) domain at fixed values of T and $u_{m1} = 2.0$, $u_{m2} = 4.0$, $u_{m3} = 6.0$.

As T increases, their profiles evolve as ring-type multisoliton pulses. They propagate outward (divergent rings) in the (X, Y, T) domain.

We note that all the above tilted ring-type multisolitons can be thought as the superposition of conic-shaped water surface and standard ring-type multisoliton. In figs. 1–3, we see that cylindrical solitons are affected by a temporal decay of their amplitudes. This intrinsic effect happens due to the geometrical character of these solutions. Therefore, we refer it to as the *physiological decay* of the cylindrical solitons. The physiological decay of a cylindrical soliton is always accompanied by the temporal growth of the pulse width. Here, we refer it to as the *physiological spreading* of the cylindrical solitons. Physiological decay and physiological spreading (flattening) are always complementary effects. From the solutions (9)–(11), we show that each ring amplitude decays as $1/T$ and the pulse width increases as $\sqrt{T}$. On the basis of these two temporal laws, the *amplitude-width* complementarity is ruled by the following law: $u_m(T)\,\sigma(T)^2 =$ constant, where $u_m(T)$ and $\sigma(T)$ are the instantaneous amplitude and width of soliton at any time, respectively. Since eq. (3) reduces to the pKdVE for very large T, this law asymptotically recovers the well-known constancy of the product $u_m\,\sigma^2$ (fixed by the coefficients of the pKdVE) that holds for planar solitons. According to eqs. (9)–(11), all multiring solitons move outward circularly with the same speed in the (X, Y, T) domain. Accordingly, we have never observed in the case of two and three solitons that a higher pulse overcomes a smaller one as it typically occurs in the case of the pKdV solitons. As a result, we conclude that the velocity of each soliton pulse or ring is independent of its amplitude. We have also never observed the breakup of a tilted localized structure (single or multisoliton) into two or more pulses and the enhancement of pulses during the spatiotemporal evolution. Nevertheless, our analytical tilted multipulse/multiring structures behave in such a way that each initial pulse/ring preserves its soliton-like shape, although the physiological variation takes place.

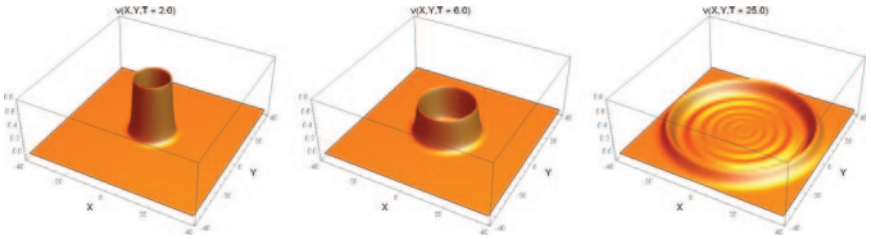

Fig. 4. – Elevation v of the numerical ring-type one-soliton solution of eq. (3) in the (X, Y, T) domain at fixed values of T satisfying the initial condition (12) and the standard boundary conditions (13). $n = 0$, $u_{m0} = 0.8$, $R_0 = 8$, and $T_{min} = 2.0$.

4. – Numerical multisoliton solution of cKdVE

Equation (3) has been solved by imposing both a multisoliton profile at the initial time $T = T_{min} > 0$, and the standard boundary conditions in (R, T) domain [12]. Then, we express the multisoliton solution v with the form of ring in the (X, Y, T) domain.

4˙1. *One-soliton solution.* – For one-soliton, eq. (3) has been solved using the initial conditions

$$v\,(R, T_{min}) = R^n\, u_{m0}\, \mathrm{sech}^2 \left[\sqrt{\frac{3\, u_{m0}}{4}}\; (R - R_0) \right], \qquad n = 0, 4, \tag{12}$$

where R_0 is an arbitrary positive constant for $n = 0, 4$. As we have used a finite-sized computational box, the standard boundary conditions are

$$v(R = 0, T) = v(R = R_{max}, T) = 0, \;\; \left.\frac{\mathrm{d}v(R,T)}{\mathrm{d}R}\right|_{R\to 0} = \left.\frac{\mathrm{d}v(R,T)}{\mathrm{d}R}\right|_{R\to R_{max}} = 0 \tag{13}$$

for R_{max} sufficiently large. Figure 4 shows the spatiotemporal evolution of the numerical ring-type one-soliton solution of eq. (3) that corresponds to the initial condition (12) with $n = 0$ and $R_0 = 8$ and the boundary condition (13) in the (X, Y, T) domain at different values of T. Furthermore, in fig. 5, we show the spatiotemporal evolution of the soliton solution in the form of multiplet that satisfies the initial condition (12) with $n = 4$ and $R_0 = 0.5$ and the boundary condition (13) in the (R, T) domain at different values of T.

4˙2. *Two- and three-soliton solutions.* – Further numerical localized solutions of eq. (3) have been found with the boundary conditions (13) and the following two- and three-soliton–like initial conditions, respectively, *i.e.*,

$$v(R, T_{min}) = (u_{m2} - u_{m1}) \frac{P + Q}{S^2}, \tag{14}$$

$$\begin{aligned} v(R, T_{min}) = P - \frac{u_{m2} - u_{m3}}{\left(\frac{u_{m1}-u_{m2}}{S} - \frac{u_{m3}-u_{m1}}{L}\right)^2} \\ \times \left[\frac{(u_{m2} - u_{m1})(P + Q)}{S^2} + \frac{(u_{m3} - u_{m1})(F - P)}{L^2} \right], \end{aligned} \tag{15}$$

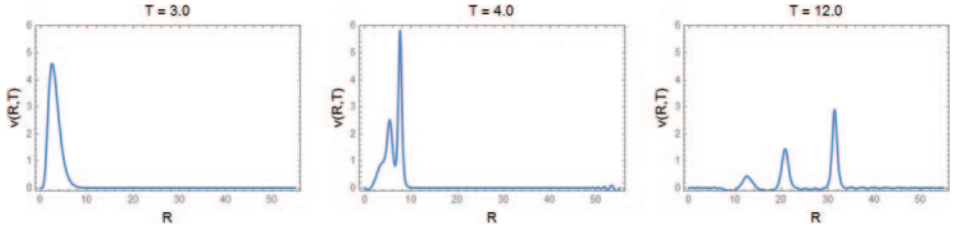

Fig. 5. – Elevation v of the numerical solution of eq. (3) *vs.* R at fixed values of T satisfying the initial condition (12) and the standard boundary conditions (13). $n = 4$, $u_{m0} = 1.0$, $R_0 = 0.5$, and $T_{min} = 3.0$.

where

$$P = u_{m1}\,\mathrm{sech}^2\left[\sqrt{\frac{3\,u_{m1}}{4}}\,(R - R_1)\right],\ Q = u_{m2}\,\mathrm{cosech}^2\left[\sqrt{\frac{3\,u_{m2}}{4}}\,(R - R_2)\right],$$

$$S = \sqrt{u_{m1}}\,\tanh\left[\sqrt{\frac{3\,u_{m1}}{4}}(R - R_1)\right] - \sqrt{u_{m2}}\,\coth\left[\sqrt{\frac{3\,u_{m2}}{4}}(R - R_2)\right],$$

$$L = \sqrt{u_{m3}}\,\tanh\left[\sqrt{\frac{3\,u_{m3}}{4}}(R - R_3)\right] - \sqrt{u_{m1}}\,\tanh\left[\sqrt{\frac{3\,u_{m1}}{4}}(R - R_1)\right],$$

$$F = u_{m3}\,\mathrm{sech}^2\left[\sqrt{\frac{3\,u_{m3}}{4}}(R - R_3)\right].$$

In the equations above, u_{m1}, u_{m2}, u_{m3}, R_1, R_2 and R_3 are positive arbitrary constants. Figures 6 and 7 show the spatiotemporal evolution of numerical ring-type two-soliton and three-soliton solution of eq. (3), respectively, in the (X, Y, T) domain at the fixed values of T. The numerical results displayed in figs. 4–7 can be summarized as follows. In figs. 4, 6, and 7, single or multiring pulses propagate outward (divergent rings) circularly in the (X, Y, T) domain, and in fig. 5, they propagate to the right in the (R, T) domain. For any time $T > T_{min}$, these initial profiles evolve as the result of their free fall and according to eq. (3). We have seen that a set of ripples appeared in the form of *water wake*. According to the terminology of the nonlinear waves, one may refer this effect to as the *radiation* of the solitonlike structures. As T increases, the amplitudes of soliton pulses decrease gradually, while the radiation tail or wake becomes longer, with increasing number of ripples. Note that the amplitude of water wake appears limited during the evolution. The amplitudes of soliton-like structures decay as T increases, but they preserve the soliton-like behavior until their amplitude is reduced almost to the same order of magnitude of the water wake. We also refer this effect to as the *physiological decay* of the pulse. The *physiological spreading* (or flattening) of pulses has been observed as T increases. Therefore, numerical results also show the complementary effects (*i.e.*, the greater amplitude the smaller width, and vice versa). In fig. 5, we show that one-soliton–like pulse, within an initially given soliton pulse, that is multiplied by powers of R, breaks up into three secondary pulses. We refer to such initial pulse as *father pulse*. We see that the father pulse has been transformed into the dominant secondary pulse (in terms of amplitude) after splitting from the smaller secondary pulses. After that,

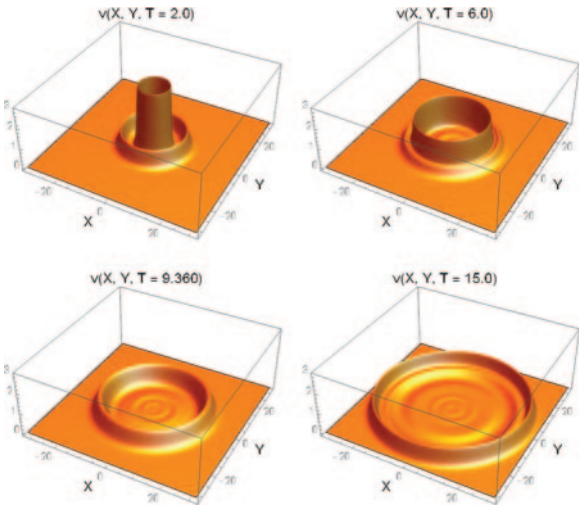

Fig. 6. – Elevation v of the numerical ring-type two-soliton solution of eq. (3) in the (X, Y, T) domain at fixed values of T satisfying the initial condition (14) and the standard boundary conditions (13). $u_{m1} = 0.8$, $u_{m2} = 3.0$, $R_1 = 11.0$, $R_2 = 6.0$, and $T_{min} = 2.0$.

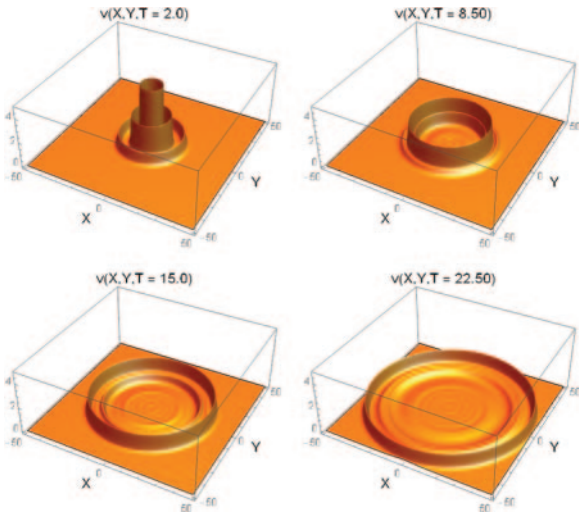

Fig. 7. – Elevation v of the numerical ring-type three-soliton solution of eq. (3) in the (X, Y, T) domain at fixed values of T satisfying the initial condition (15) and the standard boundary conditions (13). $u_{m1} = 1.0$, $u_{m2} = 2.5$, $u_{m3} = 5.0$, $R_1 = 17.0$, $R_2 = 11.0$, $R_3 = 7.0$, and $T_{min} = 2.0$.

it becomes more sharper since a part of it has created smaller pulses. During breakup process, the dominant secondary pulse becomes sufficiently sharp to enhance its amplitude which exceeds the height of the initial father pulse. This is caused due to the *maximum amplitude-width complementarity*. In figs. 6 and 7, we have seen that a higher pulse overcomes the smaller pulse. According to the above investigations, we see that

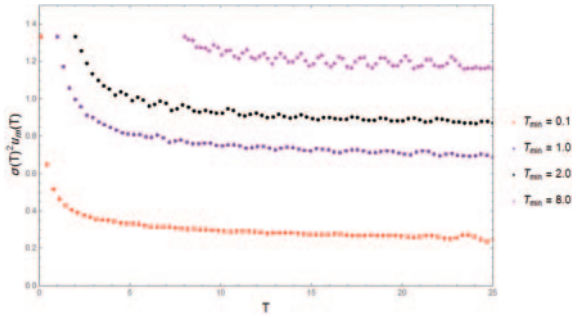

Fig. 8. – $u_m\,\sigma^2$ *vs.* T for different T_{min}. The initial profile corresponds to eq. (12) for $n = 0$, $R_0 = 8.0$, and $u_{m0} = 0.8$. Plots from bottom to top correspond to T_{min} ranging from 0.1 to 8.0.

the speed of single soliton is directly proportional to its maximum amplitude as in the planar case. All the numerical multiring solitons show the solitonlike behavior apart from the wake during the evolution. A more significant analysis has been made on the basis of single soliton solution in fig. 8. This figure displays the product $u_m(T)\,\sigma^2(T)$ of the instantaneous soliton maximum amplitude, *i.e.*, $u_m(T)$, and the instantaneous soliton width to the square, *i.e.*, $\sigma^2(T)$, for several values of T_{min}. For sufficiently large T, it is evident that the product $u_m\,\sigma^2$ becomes independent of T. This limit recovers the usual complementarity between u_m and σ of the planar case. However, during the early times, roughly, for times not exceeding $T = 10 - 15$, the cylindrical character of the solution is manifested through a violation of the constancy of this product. Of course, for large times the cKdVE reduces to the pKdVE and the constancy of the product is consistent with this limit. It turns out that σ increases when u_m decreases and viceversa, indicating the complementarity behaviour of these two quantities. Nevertheless, in the cylindrical regime, the complementary variation of these two functions do not compensate each other as in the planar case. This analysis shows the limits of previous investigations [18, 19] which did not predict the behaviour of the above product when the cylindrical character of the soliton solution is dominant during its evolution. These early works showed only the constancy of the product $u_m\,\sigma^2$, which is actually verified for larger times, only.

5. – Conclusions

In this paper, the spatiotemporal evolution of an initially given ring-type multisoliton structures in shallow water has been presented, regarding the water as inviscid, irrotational and incompressible. The spatiotemporal evolution occurs under the free fall of the initial water distribution and it is governed by the cKdVE, that has been solved both analytically and numerically. Then, the solutions have been expressed in the (R, T) domain. We have followed the evolution of localized structures along the radial direction. The solutions have also been expressed in the horizontal plane (X, Y) at each time T as 3D ring-type nonlinear waves (the vertical direction being the one of the wave elevation, *i.e.*, v). The analytical ring-type localized structures can be thought as formed on a water surface that is not initially horizontal. However, ring-type multisolitons evolve radially preserving their soliton character and the flattening of both the water surface and the pulses within the multisoliton packets takes place asymptotically. As well, ring-type multisoliton structures have been found numerically. They also evolve radially, but exhibit

a dynamics that differs substantially from the one observed for the analytical solutions. The spatiotemporal analytical multisoliton-like structures: do not exhibit overlapping of the individual pulses, because they are propagating with the same speed (this means that there is no a relationship between the pulse height and its speed); do not show any pulse splitting into two or more secondary pulses; are not accompanied by water wakes behind or ripples at the front. Conversely, the numerical multisoliton packets exhibit an internal nonlinear dynamics, very similar to the one existing in the pKdVE. Such dynamics is governed by a monotonic relationship between a soliton-like pulse and its speed. Therefore, the nonlinear character is manifested through the overcoming of a pulse of a given amplitude by the higher ones, the pulse overlapping, the pulse splitting, and the pulse radiation for the diverse initial conditions.

* * *

The author would like to thank Prof. Renato Fedele for the invaluable discussions.

REFERENCES

[1] Whitham G. B., *Linear and nonlinear waves* (John Wiley, New York) 1974.
[2] Calogero F. and Degasperis A., *Spectral transform and solitons*, vol. **I** (North-Holland, Amsterdam) 1982.
[3] Dodd R. K., Eilbeck J. C., Gibbon J. D. and Morris H. C., *Soliton and nonlinear wave equations* (Academic Press, London) 1982.
[4] Karpman V. I., *Nonlinear Waves in Dispersive Media* (Pergamon Press, Oxford) 1975.
[5] Sulem C. and Sulem P. L., *The Nonlinear Schrödinger Equation: Self-focusing and Wave Collapse* (Springer, New York) 1999.
[6] Osborne A. R., *Nonlinear Ocean Waves and the Inverse Scattering Transform* (Academic Press, Amsterdam) 2010.
[7] Nott J., *Extreme Events: A Physical Reconstruction and Risk Assessment* (Cambridge University Press, Cambridge) 2006.
[8] Onorato M. *et al.*, *Phys. Rep.*, **528** (2013) 47.
[9] Kharif C., Pelinovsky E. and Slunyaev A., *Rogue Waves in the Ocean* (Springer, New York) 2009.
[10] Synolakis C. E. and Bernard E. N., *Philos. Trans. R. Soc. A*, **364** (2006) 2231.
[11] Giancoli D. C., *Physics for scientists and engineers with modern physics*, 4th edition (Upper Saddle River, N. J., Pearson Prentice Hall) 2000.
[12] Mannan A., Fedele R., Onorato M., De Nicola S. and Jovanović D., *Phys. Rev. E*, **91** (2015) 012921.
[13] Polyanin A. D. and Zaitsev V. F., *Handbook of nonlinear partial differential equations*, 2nd edition (CRC Press, New York) 2012.
[14] Johnson R. S., *A Modern Introduction to the Mathematical Theory of Water Waves* (Cambridge University Press, Cambridge) 1997.
[15] Johnson R. S., *J. Nonlinear Math. Phys.*, **19** (2012) 1240012.
[16] Fedele R., De Nicola S., Grecu D., Shukla P. K. and Visinescu A., *AIP Conf. Proc.*, **1061** (2008) 273.
[17] Fedele R., De Nicola S., Grecu D., Visinescu A. and Shukla P. K., *AIP Conf. Proc.*, **1188** (2009) 365.
[18] Maxon S. and Viecelli J., *Phys. Fluids*, **17** (1974) 1614.
[19] Maxon S., *Phys. Fluids*, **19** (1976) 266.